

doi:10.15199/48.2024.12.40

Commutator motor fault diagnosis using acoustic data with a transfer learning approach

Streszczenie. W tym artykule, autor przedstawia nową metodę preprocessingu danych zwaną High Contrast Frequency Maps with Lowpass Filter (HCFMwLF) dla wstępnie wytrenowanych sieci neuronowych w klasyfikacji uszkodzeń silników elektrycznych. Przerwa w obwodzie wirnika, cztery wywiercone otwory w przednim łożysku, zwarcie w obwodzie stojana, uszkodzony wiatrak, uszkodzony ząb koła zębatego, uszkodzona przekładnia w porównaniu do zdrowego silnika zostały zbadane. W rezultacie, sieci GoogLeNet, ResNet-50 i VGG-19 uzyskały 100% dokładności. (Diagnostyka silników komutatorowych z wykorzystaniem danych akustycznych i transfer learning)

Abstract. In this paper, the author proposed a new method of preprocessing data called High Contrast Frequency Maps with Lowpass Filter (HCFMwLF) for the pre-trained neural networks in commutator motor fault recognition. The broken rotor coil, the four drilled holes in the front bearing, the short-circuit in stator wiring, the broken fan, the broken gear tooth and broken gear in comparison with healthy commutator motor were studied. As a result, the GoogLeNet, ResNet-50, and VGG-19 performed 100% efficiency.

Słowa kluczowe: silniki elektryczne, diagnostyka, transfer learning, uczenie głębokie.

Keywords: electric motor; diagnostic; transfer learning; deep learning.

Introduction

There are plenty of possible motor faults, both electrical and mechanical. Every kind of fault requires another approach, which can result in a relatively long time of diagnostic process. Therefore, diagnostic classification methods based on thermographic images [1, 2], vibration measurements [3, 4, 5], and audio recordings [6, 7, 8] with the usage of machine learning are becoming more and more popular every year. Acoustic signal recordings compared to vibration measuring seem to be more convenient, and similarly more convenient than using a thermal imaging camera. Sound recording requires only a smartphone or microphone with a recording device.

A variety of machine learning methods is nowadays tested with different data preprocessing approaches, to achieve possibly effective results. Denoising of the signal provides an improvement in the accuracy of models [3, 9]. Feature extraction brings significant improvement in models' accuracy by reducing data size and extracting the most important parameters. Fast Fourier Transform (FFT) is a widespread and well-established method of extracting important features of signals and is still commonly used in combination with different machine learning methods. Combining methods of denoising and feature extraction allows to obtain better efficiency of tested methods. Multivariable ensemble-based incremental SVM (MEISVM) with FFT preprocessed data performs better than bare SVM with FFT [10]. K-Nearest Neighbor (KNN), which is already in common use, tested with an Orthogonal Wavelet Transform (OTW) feature extraction performs better than the bare KNN algorithm in bearing fault recognition [5]. Support Vector Machine (SVM) with kernel principal component analysis (PCA) is increasing the performance of the SVM method in image recognition applications [11]. Noteworthy is a novel method, called Eigenclass Combination, which performs better than the following methods: Standardized Variable Distance (SVD), PS0-SVM, Probabilistic Neural Network (PNN), and Back Propagation (BP) neural network. This method achieves an accuracy of up to 100% in bearing fault recognition [12].

Deep learning has become popular and important as a result of a wide range of possible applications and high efficiency, with emphasis on Convolutional Neural Networks (CNN) and Long Short-Term Memory (LSTM) networks performances in classification. The bearing fault recognition

with Mel-CNN usage achieves 99,85% of accuracy, after windowing signal and application of FFT in dataset preprocessing [13]. Wind turbine fault recognition with LSTM provides at least comparable efficacy [14]. The combination of CNN and LSTM layers allows to obtain a higher accuracy of the model, than the separate ones [15].

However, in addition to excellent results, deep learning also has disadvantages, such as the time-consuming process of model training and the relatively huge size of the required data set for training in comparison to other machine learning methods. These problems are addressed by the transfer learning. Utilization of once trained model in another problem shortens the time of training and reduces size of necessary training set. The sound recordings of phonocardiograms of different diseases have been recognized with the usage of transfer learning networks [16]. Both audio and image processing networks can be used, with suitable preprocessing of data to sound recognition – it is a significant advantage. E. Tsalera et al. have shown, that pre-trained models for image recognition gain lower accuracy (83,97-97,22% - depending on the problem) in comparison with pre-trained for audio recognition CNNs (92,25-100%) [17]. Among the most popular transfer learning networks, we can include GoogLeNet, ResNet101, DarkNet19, AlexNet, YAMNet, and VGGish [3, 9, 17].

This paper is focused on the multiclass classification problem in commutator motor fault diagnosis with transfer learning implementation. The GoogLeNet, ResNet-50, and VGG-19 with HCFMwLF had been examined. The following faults had been diagnosed: the broken rotor coil, the four drilled holes in the front bearing, the short-circuit in stator wiring, the broken fan, the broken gear tooth and broken gear in comparison with the healthy motor of the driller.

Motor faults

The assumption behind the research is that every part of the machine participates in sound generation and produces characteristic components. Thus, faults generate their components in the audio signal spectrum. These components could be identified by appropriate software.

Single-phase commutator driller motors were examined in this research. Because of a better power-to-volume ratio than asynchronous motors, a power factor close to one and, a wide range of rotation speed regulation, this type of motor

is widely used in household appliances, many electrical tools, and electric tractions [18]. Figure 1 shows a healthy Verto electric impact drill, model 50G515, 500 W, which was used in the research.

The commutator motors consist of many elements, like a rotor with armature, commutator, brushes, stator, bearings, and others. Any part can be damaged, and this may have an impact on the exploitation of the motor, resulting in louder noise, lower torque, and effectiveness or even danger to health or even life. The break in the rotor coil is one of the faults and is shown in Fig. 2 of the examined motor. This fault affects the electromagnetic torque and rotation speed. The bearing fault may affect the inner or outer race, rolling elements, or cage. Figure 3 shows the front bearing with four drilled holes. Their defects are one of the most common among the parts of the motor. They are mainly caused by factors like temperature, the base of grease and the amount of grease, the type of bearing cage, and others. Figure 4 shows short-circuit in stator coil, which is serious threat to the machine and user. It causes a rapid increase in temperature, and a possible destruction of the engine. Figure 5 shows damaged fan, which causes abnormal cooling and increased sound intensity. Figure 6 shows broken gear tooth, and Fig. 7 shows broken gear.

Depending on the type of defect, the vibration spectrum may differ. For extended defects, changes in the signal spectrum occur on the almost entire domain of shaft speed rotation, with concentration for lower frequencies. For localized damages, mainly in higher frequencies the differences in vibration spectrum are exposed [19-21]. Using a computer with an external microphone, acoustic data from examined motors was collected. Data preprocessing and further model training are presented in section "Experiment and result".

Fig. 1. Healthy impact drill: outside (a), inside (b)

a)



b)

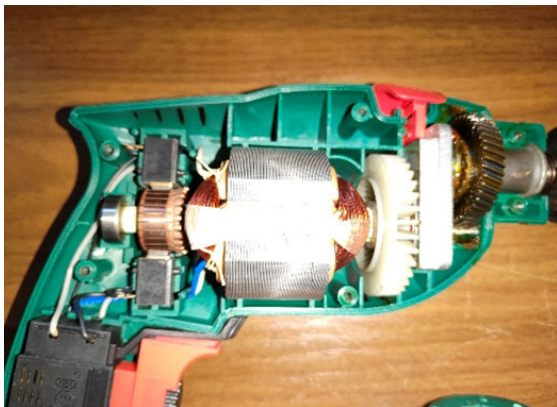


Fig. 1. Healthy impact drill: outside (a), inside (b)

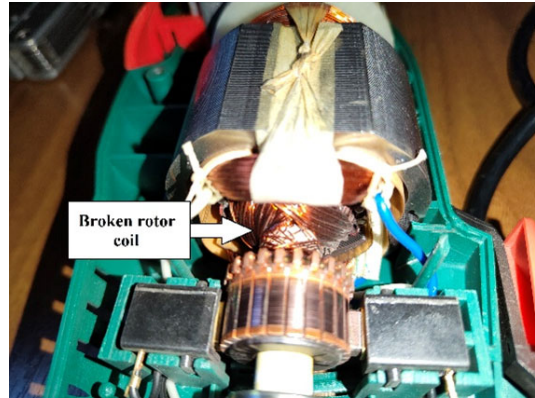


Fig. 2. The impact drill with the broken rotor coil



Fig. 3. The impact drill with the four drilled holes in the front bearing.

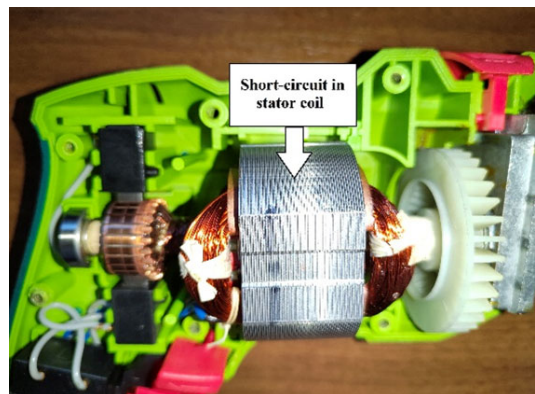


Fig. 4. The impact drill with the short-circuit in stator coil.

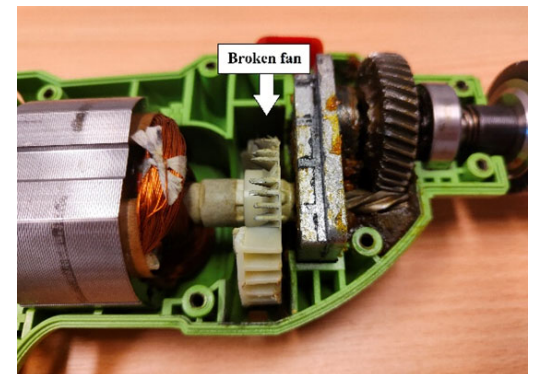


Fig. 5. The impact drill with the broken fan.

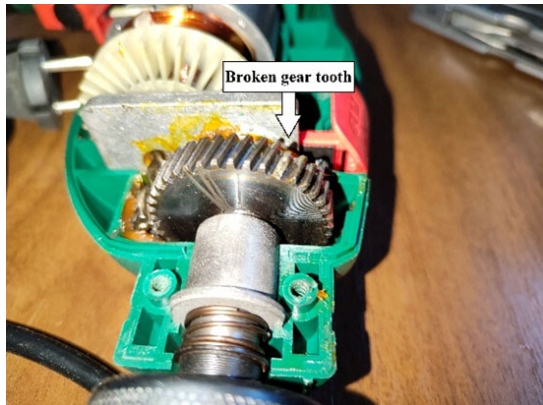


Fig. 6. The impact drill with the broken gear tooth.

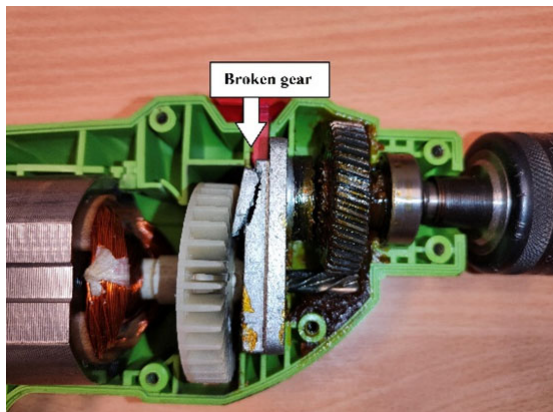


Fig. 7. The impact drill with the broken gear

Deep learning and transfer learning

In the last few decades, deep learning has become popular as a result of excellent effects in many scientific and technical fields and the availability of efficient processors. In classification problems, CNNs are often used – especially in image recognition. The advantage of CNNs lies in a reduction of required data and feature extraction. The mentioned feature extraction is an important ability of CNNs, which is provided by convolution operation (or cross-correlation, which is often implemented instead of convolution in machine learning tools). The smaller size of the kernel than the size of the entire signal (or image) allows for a reduction the number of processed data. In other words, it allows the trained model to focus on extracting the most important features in a shorter time. The particular layer (or even single neurons) of deep CNNs can specialize in extracting specific features, and sometimes it is possible to distinguish clearly which one is responsible for a specific task [22].

CNNs have been already applied in motor fault recognition. Paper [23] shows a method based on CNNs with the usage of the speed signal of a motor. Z. Gao et al. used a deep neural network with two pairs of convolutional and pooling layers, two fully connected layers, and a softmax layer. This network performed significantly better than tested RNN and LSTM in bearing fault diagnosis, especially with FFT preprocessing, which allowed Gao et al. to achieve better accuracy (85.17%) than without FFT (21.16%) in compound fault diagnosis. CNNs can also be used for diagnostics with axial magnetic flux analysis. As shown in [24] research presents the application of flux processing in fault recognition. The broken rotor bar and the stator winding fault were considered. In the mentioned research, 99.6% and 100% accuracy had been achieved. The minus of this approach is a relatively expensive and

complicated measurement system. Combining CNNs with other methods allows for an increase in the accuracy of model, which could be important in specific applications, e.g., for noisy signals. Article [25] shows multi-scale CNN with a feature attention mechanism as a solution to noisy signal classification. This method performed slightly better than others shown in the mentioned research.

Transfer learning is an approach that allows using of a once pre-trained network (or chosen layers only) to apply it for another task, especially in the case, when the training dataset is too small to train deep neural networks independently. Every layer (or group of layers) extracts features, starting with general features near the input and gradually going to specific features towards the output of the neural network. Once trained, networks could be used in a variety of ways with new datasets, relying on already obtained features. There is the possibility to choose layers (usually first n layers) to transfer from one model to another and add trainable layers on the top of the network. There are two main techniques of transfer learning, namely frozen feature extraction and fine-tuning. In the frozen feature extraction approach all layers from the base network stay unchanged and only added layers are trained to the new task. The fine-tuning allows for the unfreezing of taken layers and training them once again for the new task. A low learning rate is recommended for this method. Fine-tuning is optional in the training process, but it requires taking into consideration the overfitting problem. [26, 27].

Paper [1] shows the application of transfer learning in BLDC motor shaft diagnostic. The thermographic images were used in the training of GoogLeNet, EfficientNet-b0, and ResNet50 convolutional neural networks and 100% accuracy has been achieved in multiclassification problem. In article [9] bearing fault recognition of traction motor with GoogLeNet application has been shown. Cross wavelet transform and bandpass filter were used in denoising data, which has made it possible to increase the accuracy of models, respectively to 98.23% for a denoised signal from 89.66% for noisy signal. The research [28] shows the diagnostic framework based on transfer learning and CNNs. The proposed approach allowed to improve multitask learning CNN with fine tuning to perform up to 100% in the first case study and 94.8-98.3% in the second case study shown in the research, for preprocessed vibration signals with bispectrum-aided technique.

The GoogLeNet, ResNet-50, and VGG-19 were examined in the research. They achieved respectively 100%, 100%, and 100% of efficiency in testing set examination. The GoogLeNet, ResNet-50, and VGG-19 are CNNs pre-trained on the ImageNet database of images, prepared for categorization of 1000 classes. Respectively, they have 22, 50, and 19 convolutional layers of depth. The input size of the image is $224 \times 224 \times 3$ [29].

Experiment and result

The experiment was carried out in the room with wooden furniture. The Fifi microphone, model K669B has been used as an external microphone (frequency response: 20 – 20000 Hz, sensitivity: -34 dB), connected to the computer. The microphone was positioned 0.15 m in front of rolling parts of the driller, standing on the floor. The driller was held in my hand. The acoustic data were recorded and saved into .m4a format with 48 kHz sampling frequency, in one channel recording. The flowchart shown in Fig. 8 presents applied methods and Fig. 9 shows the flowchart of the experimental setup.

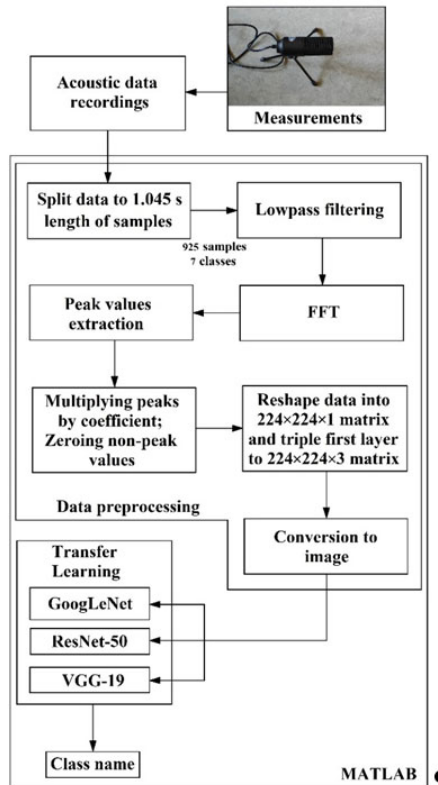


Fig. 8. Flowchart of the proposed method - High Contrast Frequency Maps with Lowpass Filter.

The raw data were preprocessed through splitting into 1.045 s samples, due to adjusting data size to neural networks input (the size of the input image for the neural networks is $224 \times 224 \times 3$; therefore, $224 \times 224 = 50176$, and divided by sampling rate of 48000 Hz gives a rounded 1.045 s). They were saved to .wav format. Next, the lowpass filter has been applied to the data samples with a passband equal to 10 kHz. This value was set based on the visible significance of occurring frequencies on FFT plots, shown in Figures 10, 12, 14, 16, 18, 20, 22. Next, the FFT method has been applied to the samples. Extracted from these spectra peaks have been multiplied by the coefficient (set to value 50 in this case), and non-peak values have been zeroed. Then, by specially written function to reshape these sample arrays, the data has been organized into $224 \times 224 \times 1$ matrixes in column-row order, one by one. After that, the first layer was tripled into the second and third layers of the image and then conversed to the .jpg image format. In this way, $224 \times 224 \times 3$ images have been obtained. The result images are shown in Figures 11, 13, 15, 17, 19, 21, 23. The images had been split into training and testing datasets. In preprocessing data and operations in neural networks, the MATLAB platform has been used.

Figures 10, 12, 14, 16, 18, 20, 22 present FFT plots with normalized amplitudes. In the time domain, it could be difficult to point out characteristic features of the signal, which allows to categorize the exact fault. Transfer of audio signal to frequency domain provides the possibility to indicate specific frequencies or features and properly categorize them. FFT is nowadays well-known and researched algorithm and in considered problem, it seems to be a sufficient transform to use in data preprocessing. With the HCFMwLF, an image from every audio sample has been generated. Every image is $224 \times 224 \times 3$ in size, according to neural network inputs.

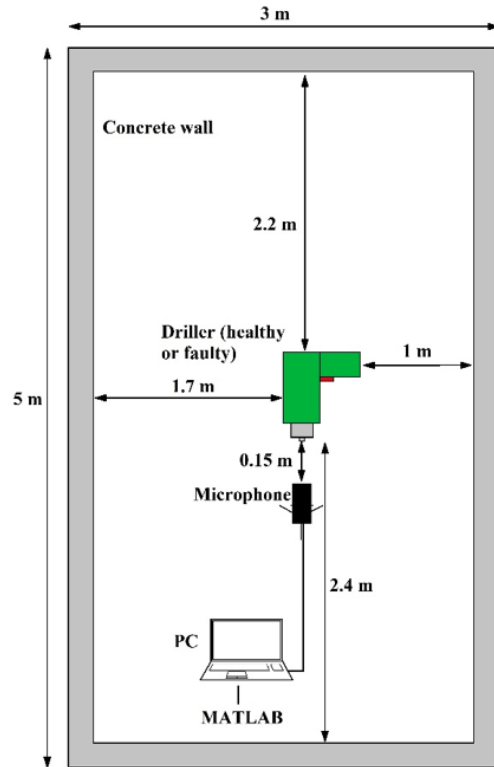


Fig. 9. The sound measurement of electric impact drill.

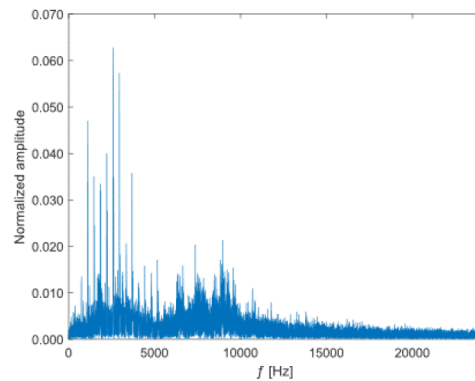


Fig. 10. FFT spectrum of analyzed healthy impact driller.

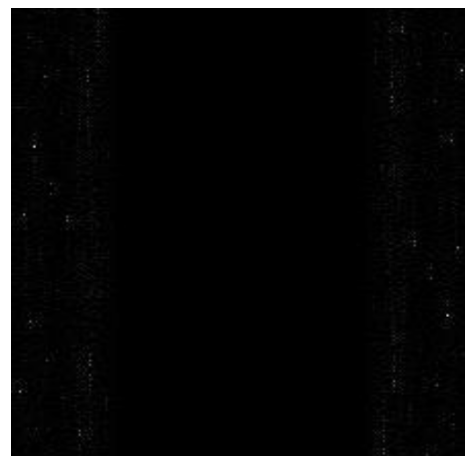


Fig. 11. HCFMwLF image of analyzed healthy impact driller.

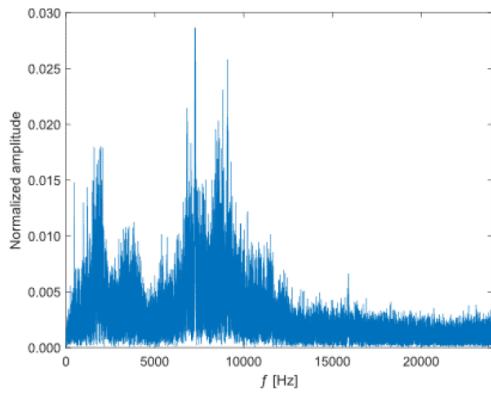


Fig. 12. FFT spectrum of analyzed impact driller with broken rotor coil.

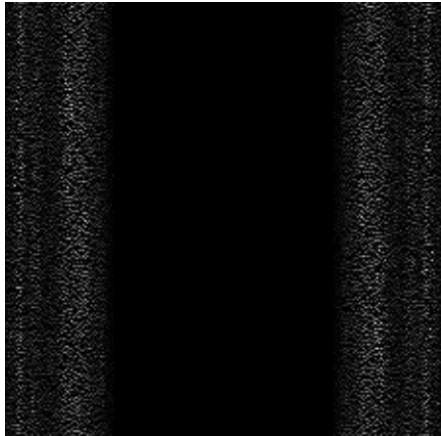


Fig. 13. HCFMwLF image of analyzed impact driller with broken rotor coil.

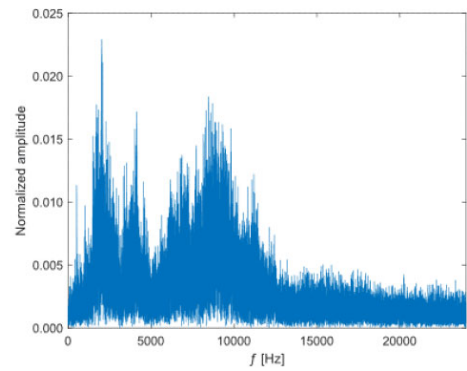


Fig. 16. FFT spectrum of analyzed impact driller with short-circuit in stator coil.

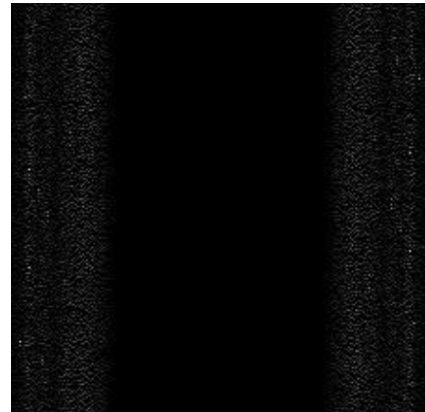


Fig. 17. HCFMwLF image of analyzed impact driller with short-circuit in stator coil.

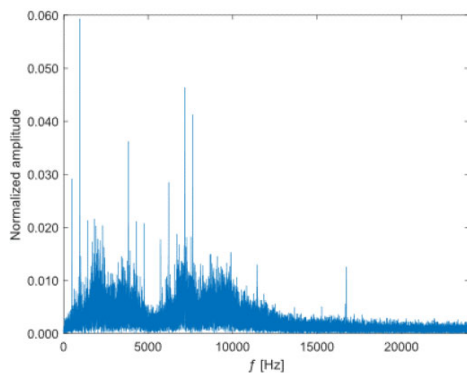


Fig. 14. FFT spectrum of analyzed impact driller with four drilled holes in front bearing.



Fig. 15. HCFMwLF image of analyzed impact driller with four drilled holes in front bearing.

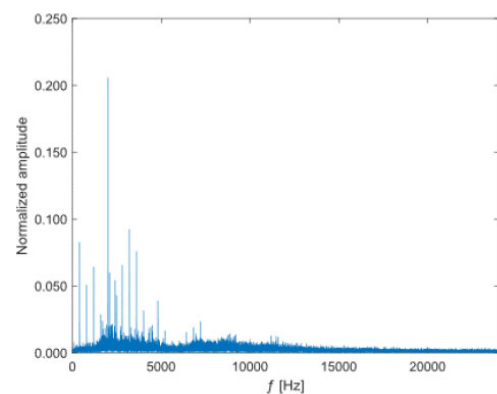


Fig. 18. FFT spectrum of analyzed impact driller with broken fan.



Fig. 19. HCFMwLF image of analyzed impact driller with broken fan.

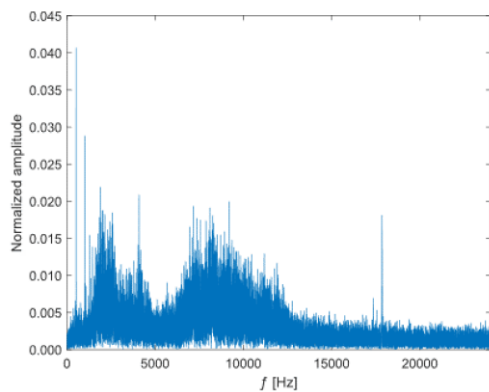


Fig. 20. FFT spectrum of analyzed impact driller with broken gear tooth.

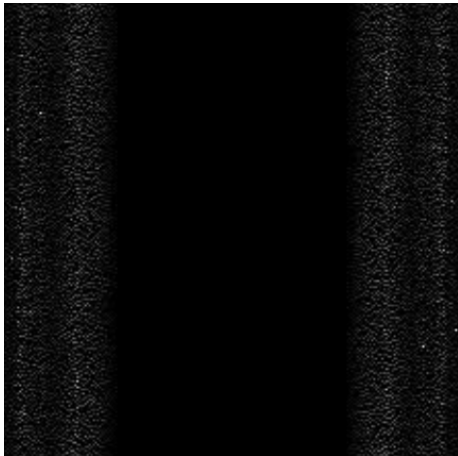


Fig. 21. HCFMwLF image of analyzed impact driller with broken gear tooth.

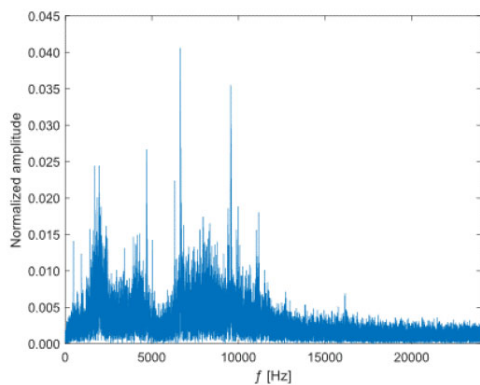


Fig. 22. FFT spectrum of analyzed impact driller with broken gear.



Fig. 23. HCFMwLF image of analyzed impact driller with broken gear.

Obtained 925 images of all classes were divided into training and testing sets. This situation is shown in Table 1. The test set constitutes 12% of the total set. The training set is balanced; therefore, it does not require downsampling and upweighting. The validation set is separated from the training set (20%).

Tabela 1. Data set structure.

Class	Training set	Test set
Broken rotor coil	121	16
Four drilled holes in the front bearing	111	15
Short-circuit in stator wiring	113	16
Broken fan	105	15
Broken gear tooth	119	16
Broken gear	120	16
Healthy	125	17
Total	814	111

The parameters of the training process for every neural network are presented in Table 2.

Tabela 2. Parameters of training for each neural network.

Parameter	GoogLeNet	ResNet-50	VGG-19
Solver	SGDM	SGDM	SGDM
Initial Learn Rate	0.0006	0.0008	0.0002
Mini Batch Size	16	12	12
Max Epochs	25	13	15
Validation Frequency	8	8	8

The comparison of chosen layers and parameters of examined networks is presented in Table 3 [29]. Because of the huge sizes of network architectures only chosen parameters have been presented. A short description is presented below.

The DAG Networks are networks organized in such a way that every layer could have multiple inputs and multiple outputs, and the DAG short comes from a Direct Acyclic Graph. GoogLeNet and ResNet-50 are DAG Networks. The series networks are networks organized layer by layer with single input and single output. The VGG-19 is a series network.

Pooling layers are often combined with convolutional layers. They are responsible for reducing the size of processed data by selecting a matrix of inputted data from the previous layer and calculating output according to the type of pooling. The Max pooling layer is a passing element whose value is the highest in the inputted matrix. Global Average Pooling does not select a matrix from the previous layer, but it calculates the average value of the size of the entire input.

The activation function layers are responsible for calculating the exact response of output based on the input. Depending on the problem, different activation functions could be used. In more demanding applications, nonlinear activation functions are preferred, such as the softmax function. This layer is often located near the output of the entire network as the final activation layer and allows for improved classification abilities of the model throughout the normalization of calculated output. The ReLU is one of the most popular activation functions used in deep learning [30]. This piecewise linear function provides more efficient and simple computations on large datasets with satisfactory outcomes.

Tabela 3. Comparison of examined networks.

Parameter	GoogLeNet	ResNet-50	VGG-19
Type	DAGNetwork	DAGNetwork	SeriesNetwork
Depth of CNN	22	50	19
Input image size	224×224×3	224×224×3	224×224×3
Convolutional layers			
Total number of layers	57	53	16
Pooling layers			
Number of Max pooling	13	1	5
Number of 2-D, Global Average Pooling	1	1	-
Activation function layers			
Number of ReLU	57	48	18
Number of Softmax	1	1	1
Normalization layers			
Number of Cross Channel Normalization	2	-	-
Number of Batch Normalization	-	53	-
Combination layers			
Number of Depth Concatenation	9	-	-
Number of Addition	-	17	-
Other layers			
Dropout	1 layer, 40% of dropout	-	2 layers, 50% of dropout
Fully Connected	1	1	1
Classification layer	1	1	1

Introducing batch normalization layers into neural networks provides increased stability of the training process and ensures shorter time. In cross channel normalization layer, the normalization is executed only along the channels.

The combination layers combine input data in the chosen way. In the addition layer, all inputs are summed up. In the depth concatenation layer, the channel dimension is distinguished as a dimension longwise in which all inputs with the same dimensions are concatenated.

The dropout layer is applied to force the specialization of non-zeroed neurons and to prevent overfitting. The fully connected layer was the layer that was replaced before the training and the number of output classes has been adjusted to four, according to the requirements of the research. Similarly, the classification layer, which is the final layer of every presented network, has been also replaced with the new one in neural network preparation.

Results

To evaluate neural networks performances, the efficiency of fault classification for every examined model has been calculated using the following ratio (1):

$$(1) \quad E = 100\% * X/Y$$

where Y is the amount of correctly classified images, and X is the amount of all tested images. The mean efficiency was calculated as a standard arithmetic mean for every model and each class. The results are presented in Tab. 4. Because the efficiency of every network for every class is 100%, there is no need to apply the F1 metric.

All examined neural networks with the HCFMwLF method performed very well. All of them: GoogLeNet, ResNet-50, and VGG-19 achieved 100% efficiency, and this is a highly satisfying result.

Tabela 4. Efficiency of examined networks.

State of motor	GoogLeNet	ResNet-50	VGG-19
	E [%]	E [%]	E [%]
Broken rotor coil	100%	100%	100%
Four holes in the front bearing	100%	100%	100%
Short-circuit in stator wiring	100%	100%	100%
Broken fan	100%	100%	100%
Broken gear tooth	100%	100%	100%
Broken gear	100%	100%	100%
Healthy	100%	100%	100%
Mean efficiency	100%	100%	100%

Conclusions

In this research, the author measured data from four classes of commutator motors of impact drillers. Seven classes: healthy motor, broken rotor coil, front bearing with four drilled holes, short-circuit in stator coil, broken fan, broken gear tooth and broken gear have been measured, processed, and classified. The author proposed a measurement experimental setup shown in Fig. 6. The conversion of acoustic records to images is an effective way to preprocess data for neural networks. The author proposed a novel method, called High Contrast Frequency Maps with Lowpass Filter (HCFMwLF) and performed further analysis. The GoogLeNet, ResNet-50, and VGG-19 have been examined. They all have reached 100% efficiency in fault classification. Image recognition with transfer learning method provided very high efficiency in researched problem. Another advantage is the short time of the training process in comparison with untrained models and smaller data set requirements. By tripling the first layer of image to the next two layers, the requirements of data amount have been decreased three times. Thus, presented in the article approach is an effective way to diagnose the exact faults of electrical motors.

Possible applications of the proposed method include diagnostics of industrial electrical tools and devices, electrical motors of cars, and in other possible areas, where electrical motors are used. Also, real time applications could be considered. Application of audio classification allows to implement early detection fault system. The acoustic data were collected with no other sounds of machines or people; thus, they were marginally contaminated by possible noises. For a larger number of devices, it would be advisable to consider acquiring audio data with microphones from each device separately and classifying the fault based on that. Also, the application of adjusted filters could be necessary.

In further research testing the HCFMwLF method with more classes could be performed. Another area of further research could focus on the application of HCFMwLF for noisy acoustic signals – it could be a successful application due to feature extraction, and suit better to the industrial environment. Also, further research could take into consideration the possibility of multifault diagnosis. For example, the case of two faults like a damaged bearing and an open circuit in rotor coil simultaneously could be considered.

REFERENCES

- [1] A. Glowacz, "Thermographic Fault Diagnosis of Shaft of BLDC Motor," *Sensors*, vol. 22, no. 21, p. 8537, Nov. 2022, doi: 10.3390/s2218537.
- [2] A. Glowacz, "Thermographic Fault Diagnosis of Ventilation in BLDC Motors," *Sensors*, vol. 21, no. 21, p. 7245, Oct. 2021, doi: 10.3390/s21217245.
- [3] Y. Yan, Q. Liu, X. qin Gao, "Motor Fault Diagnosis Algorithm Based on Wavelet and Attention Mechanism," *Journal of Sensors*, vol. 2021, p. 9, Jul. 2021. <https://doi.org/10.1155/2021/3782446>
- [4] W. Li, Y. Cao, L. Li, S. Hou, "An Orthogonal Wavelet Transform-Based K-Nearest Neighbor Algorithm to Detect Faults in Bearings," *Shock and Vibration*, vol. 2022, p. 13, Feb. 2022, <https://doi.org/10.1155/2022/5242106>
- [5] L. Wang, S. Ji, N. Ji, "Comparison of Support Vector Machine-Based Techniques for Detection of Bearing Faults," *Shock and Vibration*, vol. 2018, p. 13, Dec. 2018. <https://doi.org/10.1155/2018/8174860>
- [6] H. Nakamura, K. Asano, S. Usuda, and Y. Mizuno, "A Diagnosis Method of Bearing and Stator Fault in Motor Using Rotating Sound Based on Deep Learning," *Energies*, vol. 14, no. 5, p. 1319, Mar. 2021, doi: 10.3390/en14051319.
- [7] H. Santos, P. Scalassara, W. Endo, A. Goettel, J. Guedes, M. Gentil, "Non-invasive sound-based classifier of bearing faults in electric induction motors," *IET Science, Measurement & Technology*, vol. 15, pp. 434-445, Jul. 2021, <https://doi.org/10.1049/smt2.12044>
- [8] A. Glowacz, "Recognition of Acoustic Signals of Commutator Motors," *Applied Sciences*, vol. 8, no. 12, p. 2630, Dec. 2018, doi: 10.3390/app8122630.
- [9] G. Yang, Y. Wei, H. Li, "Acoustic Diagnosis of Rolling Bearings Fault of CR400 EMU Traction Motor Based on XWT and GoogleNet," *Shock and Vibration*, vol. 2022, p. 12, Nov. 2022. <https://doi.org/10.1155/2022/2360067>
- [10] X. Zhang, B. Wang, X. Chen, "Intelligent fault diagnosis of roller bearings with multivariable ensemble-based incremental support vector machine," *Knowledge-Based Systems*, vol. 89, pp. 56-85, Nov. 2015, <https://doi.org/10.1016/j.knsys.2015.06.017>
- [11] L. Hu, J. Cui, "Digital image recognition based on Fractional-order-PCA-SVM coupling algorithm," *Measurement*, vol. 145, pp. 150-159, Oct. 2019, <https://doi.org/10.1016/j.measurement.2019.02.006>
- [12] Z. Du, J. Ma, C. Ma, M. Huang, W. Sun, "Weighted Reconstruction and Improved Eigenclass Combination Method for the Detection of Bearing Faults", *Mathematical Problems in Engineering*, vol. 2021, p. 11, Nov. 2021. <https://doi.org/10.1155/2021/5503107>
- [13] S. Shan, J. Liu, S. Wu, Y. Shao, H. Li, "A motor bearing fault voiceprint recognition method based on Mel-CNN model," *Measurement*, vol. 207, pp. 112408, Feb. 2023, <https://doi.org/10.1016/j.measurement.2022.112408>
- [14] J. Lei, C. Liu, D. Jiang, "Fault diagnosis of wind turbine based on Long Short-term memory networks," *Renewable Energy*, vol. 133, p. 422-432, Apr. 2019, <https://doi.org/10.1016/j.renene.2018.10.031>
- [15] S. Hao, F.-X. Gao, Y. Li, J. Jiang, "Multisensor bearing fault diagnosis based on one-dimensional convolutional long short-term memory networks," *Measurement*, vol. 159, pp. 107802, Jul. 2020, <https://doi.org/10.1016/j.measurement.2020.107802>
- [16] M. Wang, B. Guo, Y. Hu, Z. Zhao, C. Liu, and H. Tang, "Transfer Learning Models for Detecting Six Categories of Phonocardiogram Recordings," *Journal of Cardiovascular Development and Disease*, vol. 9, no. 3, p. 86, Mar. 2022, doi: 10.3390/jcdd9030086
- [17] E. Tsalera, A. Papadakis, and M. Samarakou, "Comparison of Pre-Trained CNNs for Audio Classification Using Transfer Learning," *Journal of Sensor and Actuator Networks*, vol. 10, no. 4, p. 72, Dec. 2021, doi: 10.3390/jsan10040072
- [18] P. C. Sen, *Principles of Electric Machines and Power Electronics*, Chennai, India: Jon Wiley & Sons, 2013, pp. 397
- [19] R. B. Randall, J. Antoni, "Rolling element bearing diagnostics - A tutorial," *Mechanical Systems and Signal Processing*, vol. 24, issue 2, pp. 485-520, Feb. 2011, <https://doi.org/10.1016/j.ymssp.2010.07.017>
- [20] P. A. Delgado-Arredondo, D. Morinigo-Sotelo, R. A. Osornio-Rios, J. G. Avina-Cervantes, H. Rostro-Gonzalez, R. de J. Romero-Troncoso, "Methodology for fault detection in induction motors via sound and vibration signals," *Mechanical Systems and Signal Processing*, vol. 83, pp. 568-589, Jan. 2017, <https://doi.org/10.1016/j.ymssp.2016.06.032>
- [21] B. Benedik, J. Rihtaršič, J. Povh, J. Tavčar, "Failure modes and life prediction model for high-speed bearings in a through-flow universal motor," *Engineering Failure Analysis*, vol. 128, p. 105535, Oct. 2021, <https://doi.org/10.1016/j.engfailanal.2021.105535>
- [22] I. Goodfellow, Y. Bengio, A. Courville, "Convolutional Network" in *Deep Learning*, MIT Press, 2016, pp. 327-330, [Online], <https://www.deeplearningbook.org/>, accessed May 2024
- [23] Z. Guo, M. Yang, X. Huang, "Bearing fault diagnosis based on speed signal and CNN model," *Energy Reports*, vol. 8, supplement 13, p. 904-913, Nov. 2022, <https://doi.org/10.1016/j.egyr.2022.08.041>
- [24] M. Skowron, "Application of deep learning neural networks for the diagnosis of electrical damage to the induction motor using the axial flux," *Bulletin of the Polish Academy of Sciences: Technical Sciences*, vol. 68, no. 5, pp. 1031-1038, Oct. 2020, DOI: 10.24425/bpasts.2020.134664
- [25] T. Saghi, D. Bustan, and S. S. Aphale, "Bearing Fault Diagnosis Based on Multi-Scale CNN and Bidirectional GRU," *Vibration*, vol. 6, no. 1, pp. 11-28, Dec. 2022, doi: 10.3390/vibration6010002
- [26] J. Yosinski, J. Clune, Y. Bengio, H. Lipson, "How transferable are features in deep neural networks?," *arXiv: Advances in Neural Information Processing Systems 27*, pp. 3320-3328, Dec. 2014, <https://doi.org/10.48550/arXiv.1411.1792>
- [27] TensorFlow documentation, Article "Transfer learning and fine-tuning," https://www.tensorflow.org/guide/keras/transfer_learning?hl=en, accessed May 2024
- [28] M. J. Hasan, M. Sohaib, and J.-M. Kim, "A Multitask-Aided Transfer Learning-Based Diagnostic Framework for Bearings under Inconsistent Working Conditions," *Sensors*, vol. 20, no. 24, p. 7205, Dec. 2020, doi: 10.3390/s20247205
- [29] MathWorks documentation, Articles: "googlenet", "resnet50", "vgg19", <https://www.mathworks.com/>, accessed May 2024
- [30] P. Ramachandran, B. Zoph, Q. V. Le, "Searching for Activation Functions," *arXiv*, Oct. 2017, <https://doi.org/10.48550/arXiv.1710.05941>